NJC

PAPER

View Article Online
View Journal | View Issue

Cite this: *New J. Chem.*, 2016, **40**, 5722

A bistren cryptand with a remote thioether function: Cu(II) complexation in solution and on the surface of gold nanostars†

Piersandro Pallavicini,*[a] Valeria Amendola,*[a] Greta Bergamaschi,[a] Elisa Cabrini,[a] Giacomo Dacarro,[ab] Nadia Rossi[a] and Angelo Taglietti[a]

Received (in Montpellier, France) 11th November 2015,
Accepted 22nd January 2016

DOI: 10.1039/c5nj03175c

www.rsc.org/njc

A new macrobicyclic ligand capable of binding two Cu^{2+} cations has been synthesized and its protonation and coordinative properties fully determined in aqueous solution. A thioether moiety was appended on the ligand backbone. This does not influence the ligand coordination ability but allows us to graft its bis-copper complex on the surface of a self-assembled monolayer of gold nanostars (GNS), in turn grafted on glass slides pre-functionalized with a layer of a silane-bearing polyethyleneimine polymer. The release of copper ions from the GNS monolayers was also investigated, finding a general agreement with the coordination properties of the complex in solution, although the bis-copper complex displays an increased kinetic inertness when grafted on the glass slides. The photothermal properties of the GNS monolayer were studied with and without the overlayer of the Cu^{2+} complex, finding no influence of the latter but disclosing that the bis-copper complex detachment is promoted by local *T* increase due to laser irradiation.

Introduction

Bistren cryptands can be easily synthesized by Schiff base condensation and reduction of two tren (tris(2-aminoethyl)amine) molecules and three molecules of a given dialdehyde. The ellipsoidal cavity of these ligands can be varied at will, by choosing the appropriate dialdehyde as a spacer, in order to include substrates of different size and shapes.[1] Bistren ligands are able to bind two copper(II) ions with an unsaturated, distorted trigonal bipyramidal coordination geometry. The empty apical position can be exploited for the coordination of bridging anions of different kind (*e.g.* carboxylates,[2] azide,[3] halides).[4] In this paper we present a novel bistren ligand bearing a side chain with a terminal thioether functionality. Thiols, dithiols and thioethers are suitable ligands for grafting on noble metal nanoparticles[5] thanks to the strong binding interaction between sulphur atoms and *e.g.* gold and silver surfaces.

Gold nanostars (GNS) are gold nanoparticles with 2–6 branches protruding from a core and featuring the peculiar optical properties of non-spherical gold nanoparticles.[6] In particular, we recently prepared GNS using the Triton X-100 surfactant in a seed-growth approach.[7] Such GNS are characterized by two localized surface plasmon bands (LSPR) in the near IR (NIR) region of the spectrum. Both of these LSPR display an intense photothermal effect, *i.e.* once excited with a laser radiation they relax thermally, allowing the conversion of radiation into heat with a local *T* jump, and offering two photothermally active channels in a spectral region (NIR) in which blood and tissues are transparent.[7,8] The photothermal effect exerted by monolayers of GNS anchored on a surface can be exploited to obtain an antibacterial and antibiofilm action. This is triggered by through-tissues laser irradiation and opens a new approach in the surface modification of internalized medical devices (*e.g.* prostheses, implants, catheters).[9]

In addition, GNS prepared with seed-growth synthesis with TritonX-100[7] or lauryl sulfobetaine (LSB),[10] due to the weak surfactant–surface interactions can be functionalized on their surface with thiols through straight-forward mix-and-obtain procedures,[7,10,11] differently from what observed *e.g.* with gold nanorods obtained with seed-growth syntheses using strongly bonding cationic surfactants.[12] We recently exploited such property to obtain the first example of GNS co-coated with a Cu(II) complex and a stabilizing thiol (*i.e.* a thiol-terminated polyethyleneglycol)[13] and to prepare GNS co-coated with a thiolated derivative of the

[a] *Dipartimento di Chimica, Università degli Studi di Pavia, v.le Taramelli 12, 27100 Pavia, Italy. E-mail: piersandro.pallavicini@unipv.it, valeria.amendola@unipv.it; Fax: +39 0382528544; Tel: +39 0382987336, +39 0382987329*
[b] *Dipartimento di Fisica, Università degli Studi di Pavia, via Bassi 6, 27100 Pavia, Italy*

† Electronic supplementary information (ESI) available: Additional SEM and TEM images, UV-Vis-NIR extinction spectra of GNS colloidal solutions and slides, distribution diagrams for Cu^{2+}/L at micromolar concentrations. See DOI: 10.1039/c5nj03175c

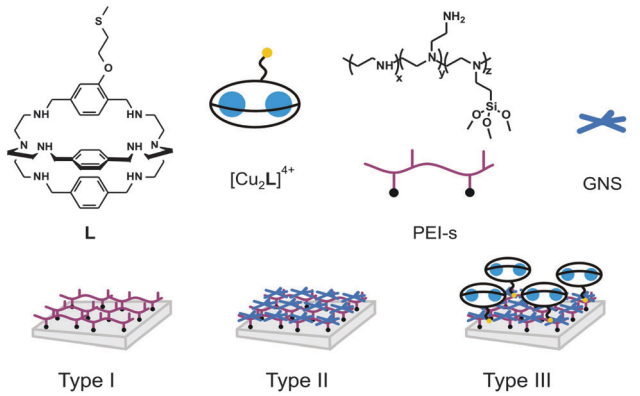

Scheme 1 Formula and schematic representation of the molecular species and surface types mentioned in this paper.

bodipy dye and with a thiol-terminated polyethyleneglycol.[14] In the latter case we also demonstrated that the thiol–gold bond can be weakened by *T* increase, so that release of a thiol-grafted molecule could be triggered also by laser irradiation, exploiting the photothermal effect.

In this paper we present GNS monolayers on glass, overcoated with the Cu(II) complex of a new bistren cryptand (**L**, Scheme 1), featuring a thiolated arm on the backbone, suitable for grafting on the GNS surface. A layer-by-layer approach was used, first coating glass slides with a siloxane derivative of the PEI (polyethyleneimine) polymer, **PEI-s**, obtaining Type I surfaces in Scheme 1. On these, we grafted GNS prepared with TritonX-100[7] (Type II surface, Scheme 1), that were further overcoated with Cu^{2+} complexes of the **L** ligand, $[Cu_2\mathbf{L}]^{4+}$, to obtain Type III surfaces. We investigated different strategies for the final step of functionalization, in order to obtain the best loading of the complex on Type II surfaces. Although papers have been published on colloidal solutions of metal nanoparticles bearing metal complexes on their surface,[15] to the best of our knowledge this is the first example of a layer-by-layer functionalization of bulk surfaces involving metal nanoparticles and transition metal complexes.

The protonation and coordination properties of **L** towards Cu^{2+} have been examined in solution by means of potentiometric titrations, and compared with the stability of the complexes as monolayers grafted on the GNS monolayer in contact with aqueous solutions, at given pH values. Moreover, the photothermal properties of the Type II and Type III surfaces have been studied. We demonstrated that the overlayer of $[Cu_2\mathbf{L}]^{4+}$ does not affect the radiation to heat conversion and that the complex release can be promoted by the local *T* jump induced by laser irradiation.

Experimental

Materials

Trimethoxysilylpropyl(polyethylenimine) (50% in isopropanol, M_w 2000–4000) was purchased from Gelest Inc. TritonX-100, tetrachloroauric acid, sodium borohydride, ascorbic acid, silver nitrate, were all purchased from Sigma-Aldrich and used without further purification. Microscopy cover glass slides (2.6 × 2.2 cm) were purchased from Forlab (Carlo Erba). All reagents for organic syntheses were purchased form Aldrich/Fluka and used without further purification. All reactions were performed under nitrogen.

Methods

Potentiometric titrations. All titrations were performed at 25.0 ± 0.1 °C. Protonation constants of ligand **L** were determined in a MeOH/water (1 : 4) mixture, 0.07 M in $NaNO_3$. In a typical experiment, 10 mL of a 7×10^{-4} M ligand solution were treated with an excess of a 1.0 M HNO_3 standard solution. Titrations were run by addition of 10 μL aliquots of carbonate-free standard 0.1 M NaOH, recording 80–100 points for each titration. Complexation constants were determined by carrying out a similar potentiometric titration experiment, with the additional presence of 2 eq. $Cu^{II}(CF_3SO_3)_2$. Prior to each potentiometric titration, the standard electrochemical potential (E°) of the glass electrode was determined in the MeOH/water (1 : 4) mixture, by a titration experiment according to the Gran method.[16] Protonation and complexation titration data (emf *vs.* mL of NaOH) were processed with the Hyperquad package[17] to determine the equilibrium constants (reported in Table 1).

In the pH-spectrophotometric titration experiment the UV-Vis absorption spectrum of the solution was recorded after each addition of standard 0.1 M NaOH.

Scanning electron microscopy (SEM). The morphologies of GNS-coated slides (see ESI,† Fig. S1) were observed under Tescan Mira XMU variable pressure Field Emission Scanning Electron Microscope – FEG SEM (Tescan USA Inc., USA). Slides were mounted onto aluminum stubs using double sided carbon adhesive tape and were then made electrically conductive by coating in vacuum with a thin layer of graphite (few nm). Observations were made in backscattered electrons mode (BSE) at 30 kV and with InBeam secondary electron detector for higher spatial resolution.

Transmission electron microscopy (TEM). GNS were coated with PEG2000-SH as described,[7] and diluted 10 times with bidistilled water. 10 μL aliquots were deposited on copper grids (300 mesh) covered with a Parlodion membrane and allowed to dry. TEM images were acquired with a Jeol JEM-1200 EX II 140 instrument.

Table 1 Logarithmic protonation and formation constants for ligand **L**

Protonated species[a]	Log *K* values[b]	Complex species[c]	Log *K* values[b]
$\mathbf{LH}_1$	9.2(1)	$\mathbf{LH}_3\mathbf{Cu}$	31.9(1)
$\mathbf{LH}_2$	17.6(1)	$\mathbf{LH}_2\mathbf{Cu}$	27.2(2)
$\mathbf{LH}_3$	25.2(1)	$\mathbf{LCu}_2$	19.0(2)
$\mathbf{LH}_4$	31.8(1)	$\mathbf{LCu}_2\mathbf{OH}$	11.8(1)
$\mathbf{LH}_5$	37.9(1)		

[a] Protonation constant of the species LH_n refers to the $L + nH^+ = [LH_n]^{n+}$ equilibrium. [b] Uncertainties in parentheses. [c] Formation constants refers to equilibria $\mathbf{L} + nH^+ + mCu^{2+} = [Cu_mH_n]^{(2m+n)+}$ (m = 1, 2; n = 0, 2, 3) The formation constant of species $\mathbf{LCu}_2\mathbf{OH}$ refers to the equilibrium $\mathbf{L} + 2Cu^{2+} + H_2O = [\mathbf{LCu}_2(OH)]^{3+} + H^+$.

Total gold and copper analysis. Each analysed slide was placed on the bottom of a 50 ml beaker and fully coated with 3.0 mL of aqua regia (diluted with bidistilled water 4 : 25 v/v). The beaker was closed with parafilm and allowed to react overnight on a reciprocating shaker, at room temperature. The blue colour of the GNS completely disappeared after few minutes, due to oxidation. The Au and Cu content was then analysed by inductively coupled plasma optical emission spectroscopy (ICP-OES), using a Optima 3000 Perkin Elmer instrument.

Analysis of copper release in water. Each analysed slide was placed on the bottom of a 50 ml beaker and fully coated with 3.0 mL of water at the chosen pH (*i.e.* 4 or 7). The beaker was closed with parafilm and allowed to react for 5 or 24 hours on a reciprocating shaker, at room temperature. After the chosen time, the glass was removed and the water acidified with 150 μL of ultrapure HNO_3. The solution was then analysed by standard techniques by ICP-OES.

Absorption and extinction spectra. Extinction spectra of colloidal suspensions were measured with a Varian Cary 100 spectrophotometer in the 200–1000 nm range or with a Cary 6000 spectrophotometer in the 300–1800 nm range. Spectra of GNS-functionalized glass slides were obtained placing the glasses on the same apparatus equipped with a dedicated Varian solid sample holder. It has to be pointed out that UV-Vis spectra of gold nanoparticles must be defined more properly as extinction spectra, as both an absorption and a scattering component contribute to the measured absorbance. UV-Vis absorption spectra of the copper complex cryptand were run on a Varian Cary 100 SCAN spectrophotometer with quartz cuvettes of the appropriate path length (0.1–1 cm) at 25.0 ± 0.1 °C under inert conditions. In any case, the concentration of the cryptand and the optical pathway were adjusted to obtain spectra with AU ∼ 1.

Photothermal behaviour. Thermograms (*T vs. t*) were recorded on glass slides of Type II and Type III by means of a laser (multimode AlGaAs laser diode, L808P200, Thorlabs GmbH, emitting light at the wavelength of about 808 nm). Temperature was recorded by means of a FLIR E40 thermocamera and FLIR Tools + software.

Syntheses

The synthesis of ligand **L** and of its precursors is sketched in Scheme 2, including H-labelling for NMR interpretation.

Synthesis of 2-[3-(methylthio)propoxy]-1,4-benzenedicarboxaldehyde (2). The dialdehyde **1** was obtained following the procedures reported in literature.[18] Reagent **2** was prepared modifying a described procedure:[19] 2-hydroxy-1,4-benzenedicarboxaldehyde (0.2 g, 1.33 mmol), K_2CO_3 (0.40 g, 2.93 mmol) and 2-chloroethyl methyl sulfide (0.26 mL, 2.66 mmol) were suspended in 5 mL DMF, and refluxed for 24 hours in inert atmosphere. The orange mixture was then cooled and filtered. 50 ml of water was added to the reaction and extracted with 5 × 50 mL of CH_2Cl_2. The collected organic phases were than washed with basic water (50 mL, 2 M NaOH), dried over Na_2SO_4 and evaporated to dryness. A yellow solid was obtained. (0.23 g, 1.06 mmol, 80%) ^{1}H NMR (400 MHz, $CDCl_3$, ppm): δ 2.2 (3H, s, Ha), 3.0 (2H, t, Hb), 4.4 (2H, t, Hc), 7.5 (2H, s, Hd, d, Hf), 8.0 (1H, d, He), 10.0 (1H, s, Hg), 10.5 (1H, s, Hh)

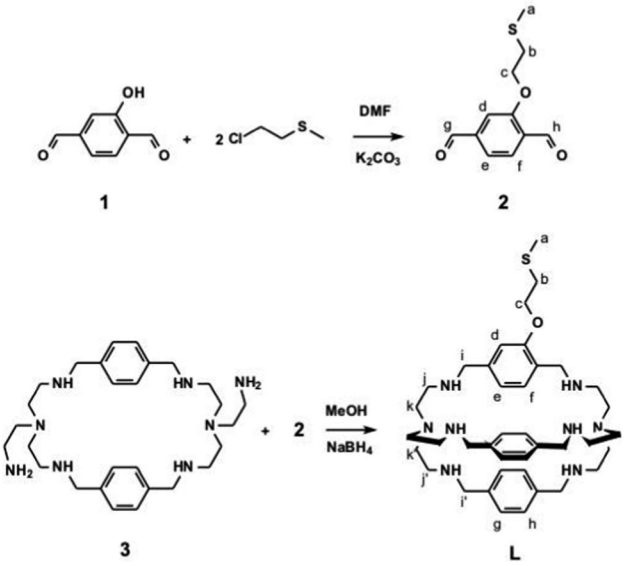

Scheme 2 Synthetic chart and labelling for ^{1}H NMR interpretation.

Synthesis of ligand L. A solution of **2** (0.12 g, 0.52 mmol) in 100 ml of MeOH was added dropwise to a stirred solution of the *p*-xylyl intermediate macrocycle **3** (0.26 g, 0.52 mmol), prepared following a published procedure[20] in 250 mL of MeOH over 3 h at room temperature. After 24 h stirring the mixture was heated to 50 °C and hydrogenated with $NaBH_4$ (0.41 g, 10.4 mmol). When the addition was complete, the reaction was stirred at 50 °C overnight. The solvent was removed and the residue was dissolved in basic water (20 mL, 1 M NaOH) and extracted with 15 ml of CH_2Cl_2 (×7). The collected organic phases were dried over Na_2SO_4 and evaporated to dryness. A white oil was obtained (0.19 g, 0.28 mmol, 54%).

MS (ESI, MeOH, pos.): *m*/*z* 345 $[M + 2H]^{2+}$, 689 $[M + H]^+$.

^{1}H NMR (400 MHz, CD_3OD, ppm): δ 2.13 (3H, s, Ha), 2.65 (12H, t br, Hj, Hj′), 2.8 (14H, m br, Hk, Hk′, Hb), 3.7 (8H, m, Hi, Hi′), 4.15 (2H, t, Hc), 6.4 (1H, d, He), 6.9 (4H, d, Hh), 7.0 (5H, m, Hf, Hg), 7.3 (1H, s, Hd).

^{13}C NMR (400 MHz, CD_3OD ppm): δ 13.5, 32.0, 52.0, 52.5, 52.7, 66.1, 110.0, 118.6, 125.5, 126.5–127.0, 137.0, 138.2, 139.3, 155.0.

Synthesis of $[Cu_2L](CF_3SO_3)_4$. To a solution of cryptand **L** (50.1 mg, 0.073 mmol) in 5 ml MeOH, 2 eq. of $Cu(CF_3SO_3)_2$ were added (53.2 mg, 0.146 mmol in 1 mL MeOH). The mixture was refluxed for 1 h. Then the solvent was concentrated and Et_2O was added. A green powder was obtained and collected by filtration. MS (ESI, MeOH, pos.): *m*/*z* 556 $[Cu_2L(CF_3SO_3)_2]^{2+}$.

GNS preparation. All the glassware used for seed-growth methods was always pretreated before use. It was washed in aqua regia for 30 min, then washed and filled with bidistilled water and ultrasonicated for 3 minutes before discarding water. The bidistilled water/ultrasound treatment was repeated 3 times. The preparation follows the general seed-growth procedure based on TritonX-100 as the protecting/directing agent, that we described elsewhere.[7]

Among the possible TritonX-100 and ascorbic acid concentrations (leading to different aspect ratios in the branches) for

this paper we used the following conditions: a seed solution was prepared in a 20 mL vial, in which 5 mL of $HAuCl_4$ 5×10^{-4} M in water were added to 5 mL of an aqueous solution of Triton X-100 0.2 M. The mixture was gently hand-shaken taking a pale yellow colour. Then, 0.6 mL of an ice-cooled solution of $NaBH_4$ 0.01 M in water were added. The mixture was gently hand-shaken and a reddish-brown colour appeared. The seed solution was kept in ice and used within 2 hours. The growth solution was prepared in a 250 mL Erlenmeyer flask. 2.50 mL of $AgNO_3$ 0.004 M in water and 50 mL of $HAuCl_4$ 0.001 M in water were added in this order to 50 mL of an aqueous solution of TritonX-100 0.2 M. Then, 1400 μL of an aqueous solution of ascorbic acid 0.0788 M were added. The solution, after gentle mixing, became colourless. After this, 120 μL of the seed solution were added. The solution was gently hand-shaken and a grey colour appeared and quickly changing to more intense and blue-black colors. The sample was allowed to equilibrate for 1 h at room temperature before using it for the coating procedures (see ESI,† Fig. S2 for an extinction spectrum). ICP-OES analysis (on ultracentrifuged pellets oxidized with aqua regia) allowed to determine the concentration of Au ($\sim$60 μg mL^{-1}, corresponding to 61% yield). Under these synthetic conditions, the extinction spectrum of such GNS presents two LSPR bands, centered at 850 and 1630 nm.

Glass slides coated with PEI (Type I surface). We slightly modified our published procedure.[21] In detail, glass substrates were first cleaned for 30 min in freshly prepared Piranha solution (3 : 1 v/v H_2SO_4 : H_2O_2 (30%). **Caution!** Piranha solution is a strong oxidizing agent and should be handled with care.), then washed three times with bidistilled water in a sonic bath and oven-dried. The slides were then immersed for 6 min in a 2% (v/v) solution of PEI-silane in ethanol at room temperature, to obtain PEI-coated slides. In a typical preparation, 5 or 8 glass slides were prepared at the same time, *i.e.* reacting in the same silane solution inside a 5-place holder (a staining jar for microscopy glass slides). After this, the slides were washed three times with ethanol and one time with ultrapure water in a sonic bath and blow-dried with nitrogen. Functionalized glasses were left to cure overnight at room temperature before use.

GNS grafted on PEI-coated slides (Type II surface). Preparation followed what we recently described.[8] Briefly, 5 or 8 slides were prepared at the same time, kept in vertical position at RT (20–25 °C) inside a 5-place or 8-place holder (a staining jar for microscopy glass slides) filled with a colloidal solutions of GNS, prepared as described in a previous section. Slides were taken off from the colloidal solutions after 18 h and appeared of a pale blue colour due to the grafted GNS monolayer. The GNS-coated slides were then washed filling the jar with bidistilled water and vigorously shaking on a reciprocating stirrer. After three washing cycles the slides were taken off and blow dried with nitrogen. They were kept in air, at room temperature, in a vertical position inside empty staining jars, under which conditions they were stable for weeks, as checked by UV-Vis extinction spectra.

$[Cu_2L]^{4+}$ grafting on Type II slides (Type III surface). Single step procedure In a typical preparation, 5 or 8 slides were prepared at the same time. Type II slides were kept in vertical position inside a 5-place or 8-place holder (a staining jar for microscopy) filled with a 10^{-4} M aqueous solution of $[Cu_2\mathbf{L}](CF_3SO_3)_4$, adjusted at pH 7 with micro-additions of 0.1 M NaOH. The slides were kept in the complex solution for 4 hours and after that were the complex solution was removed, the jar filled with bidistilled water (adjusted at pH 7) and shaken over a reciprocating stirrer for 2 min. The washing cycle was repeated three times and the slides were blow dried with nitrogen.

$[Cu_2L]^{4+}$ grafting on Type II slides (Type III surfaces). Two step procedure. In a typical preparation, 5 or 8 slides were prepared at the same time. Type II slides were kept in vertical position inside a 5-place or 8-place holder (a staining jar for microscopy) filled with a 10^{-4} M aqueous solution of **L**. The slides were kept in the ligand solution for 4 hours and after that the solution was removed and the jar filled with bidistilled water (adjusted at pH 7) and shaken over a reciprocating stirrer. The washing cycle was repeated three times and the slides were blow dried with nitrogen. In the second step the slides were immersed in a 10^{-4} M aqueous solution of $Cu(CF_3SO_3)_4$ for 4 hours, washed with water (as in the first step) and blow dried.

Results and discussion

Synthesis of ligand L

The preparation of azacryptands containing different spacer units requires a multi-step procedure, as already described by some of us in previous papers.[20,22] First, a mono protected (tris(2-aminoethyl)amine) (tren) is made to react in a 2 : 2 ratio with the a chosen dialdehyde (*p*-xylyl aldehyde in this paper), yielding an intermediate 2+2 polyimine macrocycle. After reduction with $NaBH_4$, followed by deprotection, a macrocycle featuring two pendant aminoethyl group is obtained (species **3** in Scheme 2 in our case). This is subsequently reacted in a 1 : 1 ratio with a different dialdehyde (species **2** in Scheme 2, in the present work) leading to a diimine cryptand that is reduced with $NaBH_4$ finally giving the desired aza-cryptand (**L** in Schemes 1 and 2). Dialdehydes **1** and **2** were easily obtained modifying described procedures.[18,19] By this approach, we obtained an aza-cryptand featuring an ethyl methyl sulfide chain covalently linked on one of the three *p*-xylyl spacers. R–S–R or R–S–R′ dialkyl sulphides (*i.e.* thioethers) have been reported to interact with Au flat surfaces, forming stable monolayers thanks to coordinative interactions.[23] Such monolayers are less stable than the molecular monolayers formed on Au by alkyl thiols (R–SH) and alkyl disulphides (R–S–S–R),[24] that profit of the stronger coordinative interactions between $R–S^-$ and Au^+.[25] In our case the $–CH_2–CH_2–S–CH_3$ group has been chosen as the grafting moiety in **L** due to the accessible synthetic route leading to dihaldehyde **2**. On the other hand, we did not found synthetic schemes realistically capable to lead to an azacryptand with an appended thiol or disulphide (instead of $–CH_2–CH_2–S–CH_3$).

Cu^{2+} coordination by L in aqueous solution

In order to study the acid–base behaviour of the new receptor, potentiometric titrations have been carried out on **L** in

H_2O : MeOH 4 : 1 mixture (0.07 M $NaNO_3$, at 25 °C) by addition of standard acid. The solvent mixture was used to guarantee full solubility of the ligand under all the pH values of the titration (2.5–12). Data were processed using a non-linear least-squares refinement with the HyperQuad package,[17] The obtained protonation constants are listed in Table 1.

Only five protonation constants were observed in the explored pH range, relative of five of the six secondary amines of the aza-cryptand **L** (the more hindered tertiary amines do not protonate under such conditions[20,22]). An analogous titration has been carried out in the presence of 2 equivalents of the Cu(II) salt $Cu(CF_3SO_3)_2$. The best data fitting was obtained by considering the formation of the following copper species on increasing pH: $[CuLH_3]^{5+}$, $[CuLH_2]^{4+}$, $[Cu_2L]^{4+}$ and $[Cu_2L(OH)]^{3+}$. The formation constants of such species are listed in Table 1. From the protonation and formation constants, we can calculate and draw the distribution diagram of the species in solution (% abundance with respect to total **L** *vs.* pH). This is shown in Fig. 1A. At pH 2.5, the azacryptand is in the pentaprotonated form, $[LH_5]^{5+}$ (100%). Upon addition of NaOH, the monometallic complex $[CuLH_3]^{5+}$ forms and reaches its maximum concentration (40%) at pH 4.7 (see Fig. 1A).

We may hypothesize that in $[CuLH_3]^{5+}$ the three protons are on a single tren subunit, while the second one is occupied by the Cu^{2+} ion. On increasing the pH, a proton is lost and the mononuclear copper species $[CuLH_2]^{4+}$ forms (maximum abundance 61% at pH = 5.3). The dicopper complex, $[Cu_2L]^{4+}$ is the major species in solution at pH 6.5 (75%). In $[Cu_2L]^{4+}$ each Cu^{2+} ion occupies one of the tren units, adopting the typical trigonal-bipyramidal geometry imparted by tripodal ligands.

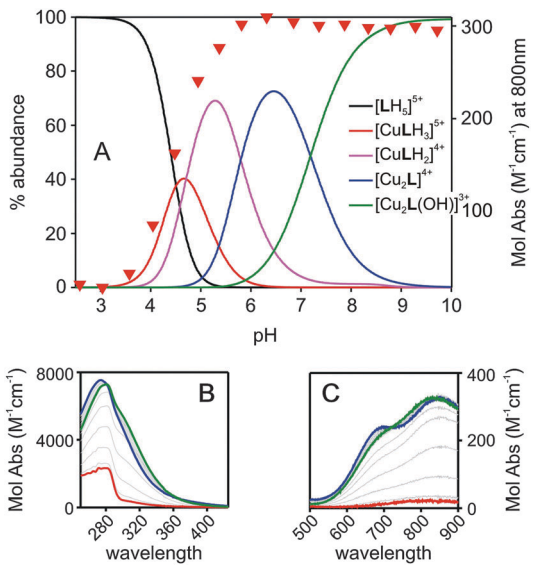

Fig. 1 (A) Distribution diagram (% of species) for the system **L**:2Cu^{2+} in H_2O : MeOH 4 : 1 (**L** = 8×10^{-4} M; $NaNO_3$ 0.07 M, 25 °C). Colour legend in the figure; (B) absorption spectra (LMCT bands, 250–400 nm range) for the same system with pH increasing from 2.4 (red spectrum) to 7.0 (green spectrum) and to 11.0 (blue spectrum). Grey thin lines are spectra taken at intermediate pH; (C) same, in the 500–900 nm range, visualizing the bands of Cu^{2+} d–d transitions.

The fifth (apical) coordination position of each metal ion is occupied by a water molecule. Upon further addition of NaOH to the complex solution, the deprotonation of the coordinated water occurs, leading to the stable hydroxide complex, $[Cu_2L(OH)]^{3+}$. Such species are typical of bis-copper complexes of bis-tren aza-cryptands, with the OH^- ion bridging between the two copper centers.[26] Due to its high stability, this species predominates in solution (>90%) over the 8–11 pH range. In addition, it has to be pointed out that from the distribution diagram it can be seen that at pH ≥ 7.0 only dicopper species exist, either as a mixture of $[Cu_2L]^{4+}$ and $[Cu_2L(OH)]^{3+}$ (7.0 < pH < 9.0) or as $[Cu_2L(OH)]^{3+}$ (pH > 9.0). Fig. 1B and C show the family of spectra taken over the course of the pH-spectrophotometric titration of a solution of **L** (0.8 mM) and $Cu(CF_3SO_3)_2$ (1.6 mM). The formation of the copper complexes is accompanied by the development of a band around 280 nm, attributable to a LMCT N(amine) → Cu(II), see Fig. 1B. Moreover, two d–d bands develop in the visible region in the 650–850 nm range (see Fig. 1C), typical of bipyramidal Cu(II) complexes.[22,26] The profile of Absorbance at 800 nm *vs.* pH (red triangles in Fig. 1A) fits well with the formation of the $[Cu_2L]^{4+}$ and $[Cu_2L(OH)]^{3+}$ species in the distribution diagram. Noticeably, the spectrum taken at pH 7 (blue lines in Fig. 1B and C, maximum% of $[Cu_2L]^{4+}$) and at pH 11 (green lines in Fig. 1B and C, 100% $[Cu_2L(OH)]^{3+}$) show slight but sharp differences, evidencing the different coordinative sphere of the Cu^{2+} cations between the two species.

Formation of GNS monolayer and $[Cu_2L]^{4+}$ grafting

The formation of a polyethyleneimine layer on glass using PEIs (Type I surface in Scheme 1) has been already reported by us.[8,21] Such a layer has a 1–2 nm thickness, *i.e.* the polymer lies flat on the surface. Type I surfaces can form monolayers of silver nanospheres[8] and of GNS[21] thanks to electrostatic interactions between the protonated polyamine network and the negatively charged nanoparticles surface. In the GNS case (Type II surfaces in Scheme 1) we also explored the kinetics of coating.[21] By dipping Type I slides in GNS colloidal solutions for different times we observed a linear increase of the GNS density on the surface, turning into a plateau after 16 h. In the present work we used colloidal solutions of GNS prepared with the same seed-growth synthesis (TritonX-100 as protecting and directing agent[7]), see Fig. 2A for a TEM image. The chosen conditions are such to have the first NIR LSPR absorption band centred at ~860 nm (see ESI,† Fig. S2) in the colloidal solution. This is a slightly longer wavelength with respect to the GNS used to prepare Type II slides in ref. 7. The second LSPR is at 1630 nm in the colloidal solution.

Au concentration in the GNS colloidal solution is 60 μg mL^{-1} (61% conversion yield from $AuCl_4^-$), calculated separating GNS from solution by ultracentrifugation and analysing the obtained pellet by ICP-OES after full oxidation in a given volume of aqua regia. Grafting GNS on PEI causes a ~50 nm blue shift of the first LSPR (and a ~300 nm blue shift of the second one), due to the well-known sensitivity of LSPR bands to the local refractive index. The latter changes from 1.3339 (water)

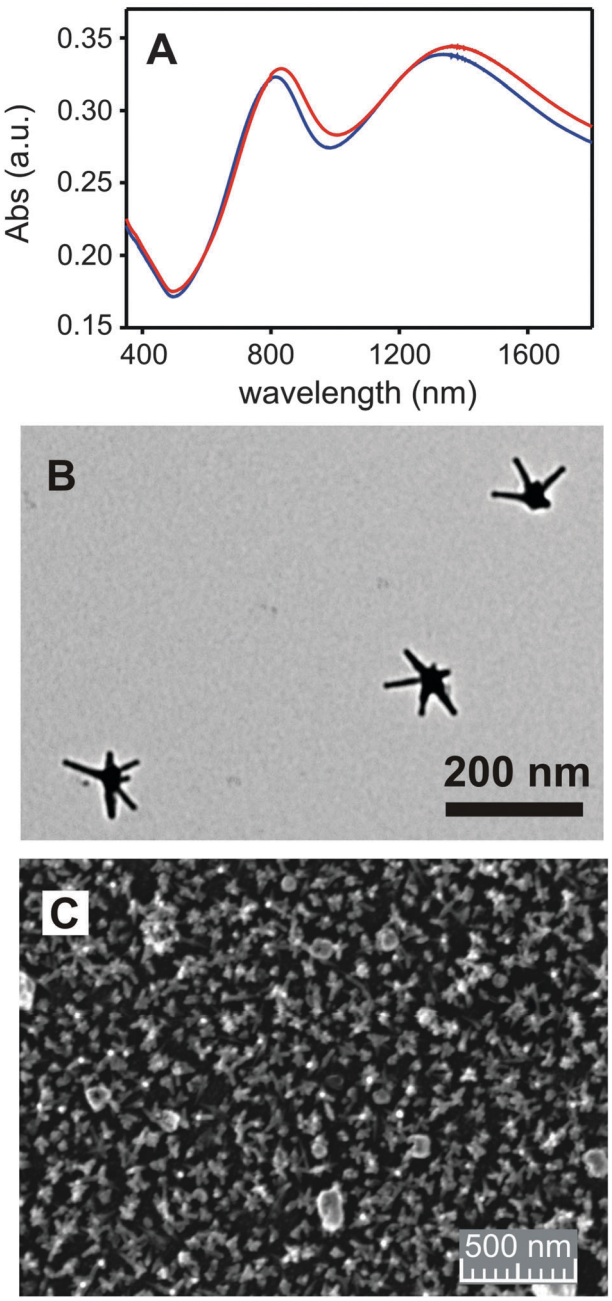

Fig. 2 (A) Extinction spectra of Type II surface (blue color) and of Type III surface obtained from it (red color); (B) TEM image of a GNS used for coating (see ESI,† Fig. S3 for complete image); (C) SEM image of a Type II surface (particular; see ESI,† Fig. S1 for full image and additional images).

in colloidal solution to that of a mixed medium composed mainly of air (1.0003) and of PEI (on which the GNS are adhering). The wavelength maximum of the first LSPR in solution is chosen in order to obtain an absorption maximum at ~800 nm on Type II surfaces (see Fig. 2B, blue line). This is the wavelength of the laser source available in our laboratories. We used 18 h dipping time to prepare Type II surfaces, to be sure to obtain the maximum surface coating. Gold content was determined by full oxidation of the GNS monolayer with aqua regia and standard analysis by ICP-OES. An average of 4.7(±0.3) μg Au per cm was found on 3 different preparations, in agreement with what observed previously for the same GNS but with lower aspect ratio of the branches (first LSPR at 630 nm, second at 1100 nm when grafted on glass in ref. 7). SEM imaging, Fig. 2C, show a homogeneous distribution of the GNS lying flat on the surface, forming a (sub)monolayer. Due to their irregular shape, close packaging of GNS is obviously not allowed and unoccupied space is left on the surface. Note that the less sharp GNS morphology in the SEM image is due to the coating with ~5 nm of sputtered graphite, added to ensure the necessary sample conductivity.

Type III surfaces feature an additional overlayer of the bis-Cu^{2+} complex of cryptand **L**. To obtain such surfaces we have used a two-step approach (TSA) and a single-step approach (SSA). In the TSA, the empty ligand is first grafted on the free surface of GNS by dipping Type II glass slides in a 10^{-4} M aqueous solution of **L**. Slides were then repeatedly washed (see Experimental) to remove the **L** ligand not grafted on the surface. Finally they were immersed in a 10^{-4} M solution of Cu^{2+} (as its triflate salt) for 4 hours, then repeatedly washed with bidistilled water. ESI† (Fig. S4a) reports the extinction spectra of the starting surface (Type II) and of the two steps. With the SSA, the $[Cu_2\mathbf{L}](CF_3SO_3)_2$ complex was instead pre-prepared and isolated as described in the Experimental. Type II slides were immersed for 4 h in a 10^{-4} M solution of such complex, regulated at pH 7 by NaOH microadditions, and then repeatedly washed with bidistilled water. With both approaches the LSPRs of the GNS shifted significantly to the red, indicating a change of the local refractive index around GNS.[27] Interestingly, with the TSA we observed first a small red shift when the empty ligand was added, and then an additional, more significant red shift when Cu^{2+} was added to the modified surfaces, see Table 2 and ESI† (Fig. S4A). In the case of SSA, the observed red shift is instead smaller than that observed after the second step of the TSA (Table 2). Fig. 2A displays the extinction spectrum of Type III surface prepared with SSA (red spectrum), evidencing such red shift. ICP-OES analysis was carried out to determine the total quantity of Cu^{2+} on the surface after the two approaches. Data are collected in Table 2 and show that the TSA yields surfaces with a significantly lower quantity (63% lower) of Cu^{2+} with respect to the SSA preparations. A larger $\Delta\lambda$ shift is observed in the TSA, particularly in the second step, when Cu^{2+} is added to the surface with grafted but void ligand **L**. This observation and the found low Cu^{2+} surface concentration

Table 2 LSPR wavelength shift and Cu surface concentration

Synthetic approach	$\Delta\lambda$ (LSPR1)[a]	$\Delta\lambda$ (LSPR2)[b]	Cu^{2+} per cm
TSA[c]	29 nm 1st 6 nm(±2) 2nd 23 nm(±7)	30 nm 1st 12 nm(±4) 2nd 18 nm(±8)	0.13(0.03) nmol cm^{-2}
SSA[d]	17 nm(±8)	31 nm(±14)	0.35(0.05) nmol cm^{-2}

[a] LSPR1 is the LSPR at ~800 nm for Type II surfaces. [b] LSPR2 is the LSPR at ~1350 nm for Type II surfaces. [c] Data on 6 slides from two different preparations. [d] Data on 32 slides from 4 different preparations.

suggest that the added free Cu^{2+} cations interact with the GNS environment, but do not enter (or enter just in small percent) inside the surface-confined bis-tren cage. Complexation to the free portions of PEIs can be hypothesized, as glass-grafted PEIs has already been proven to weakly bind Cu^{2+} from aqueous solutions.[21] Experiments carried out immersing the Type II surfaces in 10^{-4} M $Cu(CF_3SO_3)_2$ support such hypothesis, as similar shifts of the LSPR bands are observed (ESI,† Fig. S4B). This picture is not surprising, considering the already observed surface kinetic effect, hugely slowing the complexation/decomplexation processes taking place on ligands grafted at a short distance to a bulk surface.[28] On the other hand, the SSA employs the preformed $[Cu_2\mathbf{L}](CF_3SO_3)_4$ complex and leads to higher Cu^{2+} surface concentrations. The obtained $\sim$0.35 nmol Cu^{2+} per cm concentration corresponds to a $\sim$0.175 nmol cm^{-2} concentration of $[Cu_2\mathbf{L}]^{4+}$.[29] This value is well inscribed inside what found for molecular monolayers of Cu^{2+} complexes grafted by a pendant function on flat glass. Examples are the Cu^{2+} complex of a tetraaza macrocyclic ligand (0.22 nmol cm^{-2}) and of the 2,2-bipyridine ligand (0.17 nmol cm^{-2}).[28] In the present case the surface offered for grafting $[Cu_2\mathbf{L}]^{4+}$ is of course different from a flat glass slide, as it is made of GNS in turn grafted on glass. Such surface has a nanostructured shape capable of increasing the available surface: an higher surface concentration of grafted complex could be expected. On the other hand the GNS monolayer on Type II surfaces is not densely packed, see Fig. 2C, and this lowers the surface concentration of the grafted complex. On the basis of these data, the SSA has been used in all subsequent studies.

The stability of the grafted complexes has been checked by Cu^{2+} release in water from Type III surfaces. This has been done by dipping the washed and dried slides in a small volume of water, with the pH adjusted at the two representative values 4.0 and 7.0, for immersion times of 5 h and 24 h (ICP-OES analysis of copper followed). Releasing Cu^{2+} in water from a surface after washing it with the same solvent seems apparently contradictory, as larger volumes of water are used in the washing process and extensive Cu^{2+} decomplexation may be hypothesized. However metal cations actually remain on the surface after washing, as demonstrated also by total Cu^{2+} data in Table 2. This happens thanks to the already mentioned kinetic effect played by the surface, behaving as an ''infinite dimension'' substituent, that enhances the sluggishness of the release process.[28] The % Cu^{2+} release has been calculated on the basis of total copper determined by oxidation with HNO_3 on samples coming from the same preparations. To evaluate the expected release at the equilibrium, we can use the formation constants of Table 1 and calculate what would be the free Cu^{2+} cation if all the grafted $[Cu_2\mathbf{L}]^{4+}$ complex was considered as dissolved in 3.0 mL of water (the volume used for release). Under these conditions, at pH 7.0 the 32% of copper would be free (and 68% bound to **L** as a mixture of $[Cu\mathbf{L}H_2]^{4+}$, $[Cu_2\mathbf{L}]^{4+}$ and $[Cu_2\mathbf{L}(OH)]^{3+}$, see ESI,† Fig. S5 for details). This fits reasonably well with the found 38($\pm$18)% release after 24 h. The lower release at 4 h, 16($\pm$8)%, gives instead account of the enhanced kinetic inertness of the complexation and decomplexation processes on a ligand bound to a surface by a short dangling arm. On the other hand, the same calculation carried out at pH 4.0 give 100% of expected free Cu^{2+}. Actually we found significantly higher % of released Cu^{2+} with respect to pH 7.0, *i.e.* 60($\pm$6)% after 4 h and 72($\pm$17)% after 24 h. The incomplete release at lower pH was not further investigated, and can be attributed to the different environment for **L** between solution and surface, that may lead not only to different observed complexation constants but also to different local H^+ concentration.

The photothermal behaviour of Type II and Type III slides has been measured by irradiation with a 800 nm continuous laser source (200 mW, spot diameter 1 cm) on 1 $\times$ 1 cm glass slides. These were obtained by cutting the larger slides typically used for synthesis. Thermograms (ΔT *vs.* t) were recorded with a thermocamera, observing in all cases an increase-plateau profile, reaching the plateau within 40 seconds, see Fig. 3. The presence of a monolayer of $[Cu_2\mathbf{L}]^{4+}$ does not influence the photothermal response, as it can be seen comparing Fig. 3A (Type II surface) and Fig. 3B (Type III surface). Plateau values of 19.6(5) °C and 19.1(8) °C, respectively, were obtained. For measurements we irradiated a Type II slide, then coated it with SSA to obtain a Type III slide, then we used this for irradiation. No difference is observed despite the $[Cu_2\mathbf{L}]^{4+}$ absorption at 800 nm. This is due to the dramatically different extinction coefficient of the Cu^{2+} d–d band ($<$300 M^{-1} cm^{-1}, see Fig. 2C) with respect to that of the bands due to LSPR in gold nanoparticles.[6,13] Finally, we irradiated glass slides of Type III ($\sim$1 cm^2) immersed in 0.500 mL of water at pH 7.0. Irradiation was carried on for 0.5 hours and the obtained water solution collected and analyzed. We observed that in this case the Cu^{2+} concentration in the release solution was 20% of the total Cu^{2+} (compared by ICP-OES Cu^{2+} analysis on Type III slides of the same preparation treated with HNO_3 for full copper release). Such % value is higher than the % release observed after 4 h at pH 7.0 in water with no laser irradiation. Although a faster decomplexation of Cu^{2+} from **L** could also be considered, due to the increased local temperature, the 20% Cu^{2+} release value observed in 0.5 hours with laser irradiation, compared to the 16% release in 4 h (no laser), points towards a different explanation. In the laser irradiation case, the detachment of

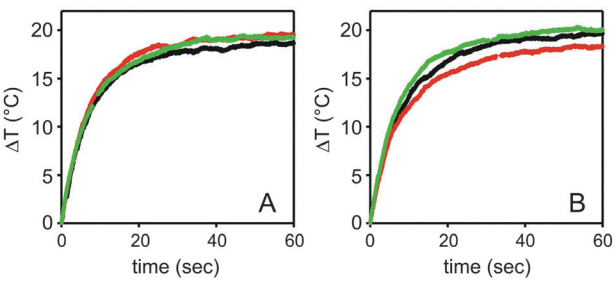

Fig. 3 (A) Thermograms (ΔT *vs.* t) for Type II surfaces, obtained by irradiation at 800 nm with a 200 mW laser source on a 1 cm diameter spot (irradiance = 0.25 W cm^{-2}). The three profiles refer to three different slides from the same preparation. (B) Same as A, for Type III surfaces. The profiles with the same colour are from the same slide, before (A) and after (B) coating with $[Cu_2\mathbf{L}]^{4+}$.

the whole $[Cu_2\mathbf{L}]^{4+}$ complex has to be hypothesized: local *T* increase on GNS surface by photothermal conversion of laser irradiation has already been recently demonstrated capable of promoting breaking of gold–sulphur bonds,[14] similarly to what described also on gold nanorods.[30]

Conclusions

The new bis-tren cryptand **L** has been prepared and its coordinative properties towards Cu^{2+} fully determined in aqueous solution, revealing the expected similarities with analogous bis-tren cage ligands.[26] However, the used synthetic strategy allowed to obtain such ligand with a thioether dangling arm on its backbone. This has no influence on the ligand coordinative properties but is an efficient anchoring function for preparing a monolayer of its Cu^{2+} complex on gold nanostars. These were in turn grafted on a bulk glass surface functionalized with a polyethyleneimine polymer equipped with trimethoxysilane functions. On the basis of released Cu^{2+} cation from the surface–grafted complexes at pH 7.0 and 4.0, we can also hypothesize that the coordinative properties of the cage ligand are approximately retained when it is confined on the GNS surface on glass slides. However, a significant kinetic inertness is introduced by the "infinite dimensions" of the surface. Moreover, also the photothermal properties of the gold nanostars monolayer are retained after functionalization with the bis-copper complex of **L**. It was also observed that irradiation of gold nanostars on their near-IR LSPR promotes the release of the whole complex, due to the local *T* increase that weakens the S–Au bond. As a proof of concept, Type III surfaces thus indicate that it is possible to prepare highly stable Cu^{2+} complexes and graft them on a surface with no cation lost. Then it is also possible either to induce a slow Cu^{2+} release by a pH change (*e.g.* switching from the physiological pH range to a mildly acidic one) or to promote the whole complex release by an external switch (laser irradiation in the near-IR). Such surfaces may be prototypes for antibacterial switchable materials *e.g.* for prostheses, in which the contact with a bacterial colony with acidic metabolism induces the release of an antibacterial cation (Cu^{2+}),[28] and whose action can be coupled with local hyperthermia[9] by laser irradiation, in a wavelength range (near-IR) in which tissue and blood are transparent.

Acknowledgements

Funding: we thank MIUR (PRIN 2010-2011, 20109P1MH2_003) and Università di Pavia (grant Fondo Ricerca Giovani for E. Cabrini).

Notes and references

1 J.-M. Lehn, S. H. Pine, E. Watanabe and A. K. Willard, *J. Am. Chem. Soc.*, 1977, **99**, 6766; G. Alibrandi, V. Amendola, G. Bergamaschi, L. Fabbrizzi and M. Licchelli, *Org. Biomol. Chem.*, 2015, **13**, 3510–3524.
2 M. Boiocchi, M. Bonizzoni, L. Fabbrizzi, G. Piovani and A. Taglietti, *Angew. Chem., Int. Ed.*, 2004, **43**, 3847.
3 F. A. Mautner, C. N. Landry, A. A. Gallo and S. S. Massoud, *J. Mol. Struct.*, 2007, **837**, 72.
4 V. Amendola, E. Bastianello, L. Fabbrizzi, C. Mangano, P. Pallavicini, A. Perotti, A. Manotti Lanfredi and F. Ugozzoli, *Angew. Chem., Int. Ed.*, 2004, **39**, 2917–2920.
5 H. Groenbeck, A. Curioni and W. Andreoni, *J. Am. Chem. Soc.*, 2000, **122**, 3839–3842; E. C. Hurst, K. Wilson, I. J. S. Fairlamb and V. Chechik, *New J. Chem.*, 2009, **33**, 1837–1840.
6 A. Guerrero-Martìnez, S. Barbosa, I. Pastoriza-Santos and L. M. Liz-Marzàn, *Curr. Opin. Colloid Interface Sci.*, 2011, **16**, 118–127.
7 P. Pallavicini, A. Donà, A. Casu, G. Chirico, M. Collini, G. Dacarro, A. Falqui, C. Milanese, L. Sironi and A. Taglietti, *Chem. Commun.*, 2013, **49**, 6265–6267.
8 P. Pallavicini, S. Basile, G. Chirico, G. Dacarro, L. D'Alfonso, A. Donà, M. Patrini, A. Falqui, L. Sironi and A. Taglietti, *Chem. Commun.*, 2015, **51**, 12928–12930.
9 P. Pallavicini, A. Donà, A. Taglietti, P. Minzioni, P. Pallavicini, A. Donà, A. Taglietti, P. Minzioni, M. Patrini, G. Dacarro, G. Chirico, L. Sironi, N. Bloise, L. Visai and L. Scarabelli, *Chem. Commun.*, 2014, **50**, 1969–1971.
10 P. Pallavicini, G. Chirico, M. Collini, G. Dacarro, A. Donà, L. D'Alfonso, A. Falqui, Y. A. Diaz-Fernandez, S. Freddi, B. Garofalo, A. Genovese, L. Sironi and A. Taglietti, *Chem. Commun.*, 2011, **47**, 1315–1317.
11 (*a*) A. Casu, E. Cabrini, A. Donà, A. Falqui, Y. Diaz-Fernandez, C. Milanese, A. Taglietti and P. Pallavicini, *Chem. – Eur. J.*, 2012, **18**, 9381; (*b*) H. Yuan, C. G. Khoury, H. Hwang, C. M. Wilson, G. A. Grant and T. Vo-Dinh, *Nanotechnology*, 2012, **23**, 075102.
12 K. G. Thomas, S. Barazzouk, B. I. Ipe, S. T. S. Joseph and P. V. Kamat, *J. Phys. Chem. B*, 2004, **108**, 13066–13068.
13 P. Pallavicini, C. Bernhard, G. Chirico, G. Dacarro, F. Denat, A. Donà, C. Milanese and A. Taglietti, *Dalton Trans.*, 2015, **44**, 5652–5661.
14 M. Borzenkov, G. Chirico, L. D'Alfonso, L. Sironi, M. Collini, E. Cabrini, G. Dacarro, C. Milanese, P. Pallavicini, A. Taglietti, C. Bernhard and F. Denat, *Langmuir*, 2015, **31**, 8081–8091.
15 (*a*) X. Sun, R. Rossin, J. L. Turner, M. L. Becker, M. J. Joralemon, M. J. Welch and K. L. Wooley, *Biomacromolecules*, 2005, **6**, 2541; (*b*) A. I. Jensen, T. Binderup, P. E. K. Kumar, A. Kjær, P. H. Rasmussen and T. L. Andresen, *Biomacromolecules*, 2014, **15**, 1625.
16 (*a*) G. Gran, *Analyst*, 1952, **77**, 661–771; (*b*) P. Gans and B. O'Sullivan, *Talanta*, 2000, **51**, 33–37.
17 P. Gans, A. Sabatini and A. Vacca, *Talanta*, 1996, **43**, 1739–1753; http://www.hyperquad.co.uk/index.htm; accessed on July 25, 2009.
18 T. Ise, D. Shiomi, K. Sato and T. Takui, *Chem. Mater.*, 2005, **17**, 4486–4492.
19 C. L. Yeung, S. Charlesworth, P. Iqbal, J. Bowen, J. A. Preece and P. M. Mendes, *Phys. Chem. Chem. Phys.*, 2013, **15**, 11014–11024.

20 V. Amendola, G. Bergamaschi, M. Boiocchi, R. Alberto and H. Braband, *Chem. Sci.*, 2014, **5**, 1820–1826.
21 G. Dacarro, L. Cucca, P. Grisoli, P. Pallavicini, M. Patrini and A. Taglietti, *Dalton Trans.*, 2012, **41**, 2456–2463.
22 G. Bergamaschi, M. Boiocchi, M. L. Perrone, A. Poggi, I. Viviani and V. Amendola, *Dalton Trans.*, 2014, **43**, 11352.
23 J. C. Love, L. A. Estroff, J. K. Kriebe, R. G. Nuzzo and G. M. Whitesides, *Chem. Rev.*, 2005, **105**, 1103–1169.
24 (*a*) C. Jung, O. Dannenberger, Y. Xu, M. Buck and M. Grunze, *Langmuir*, 1998, **14**, 1103–1107; (*b*) E. B. Troughton, C. D. Bain, G. M. Whitesides, R. G. Nuzzo, D. L. Allara and M. D. Porter, *Langmuir*, 1988, **4**, 365–385.
25 (*a*) R. G. Nuzzo, L. H. Dubois and D. L. Allara, *J. Am. Chem. Soc.*, 1990, **112**, 558–569; (*b*) T. P. Gustafson, Q. Cao, S. T. Wang and M. Y. Berezin, *Chem. Commun.*, 2013, **49**, 680–682.
26 V. Amendola, L. Fabbrizzi, C. Mangano, P. Pallavicini, A. Poggi and A. Taglietti, *Coord. Chem. Rev.*, 2001, **219**, 821–837.
27 P. Pallavicini, C. Bernhard, G. Dacarro, F. Denat, Y. A. Diaz-Fernandez, C. Goze, L. Pasotti and A. Taglietti, *Langmuir*, 2012, **28**, 3558–3568.
28 P. Pallavicini, G. Dacarro, Y. A. Diaz-Fernandez and A. Taglietti, *Coord. Chem. Rev.*, 2014, **275**, 37–53.
29 The $[Cu_2\mathbf{L}]^{4+}$ formula is written in this part of the paper for sake of simplicity. Although the grafting process of the preformed complex has been carried out at pH 7, at which value $[Cu_2\mathbf{L}]^{4+}$ is the prevalent species in water, we are not able to calculate the complexation constants of the ligand L grafted on surface, and at pH 7 the complex may as well exist on surfaces as a mixture with $[Cu_2\mathbf{L}(OH)]^{3+}$.
30 G. Gonzalez-Rubio, J. Gonzalez-Izquierdo, L. Bañares, G. Tardajos, A. Rivera, T. Altantzis, S. Bals, O. Peña-Rodríguez, A. Guerrero-Martínez and L. M. Liz-Marzán, *Nano Lett.*, 2015, **15**, 8282–8288.

